ADVANCED FUNCTIONAL MATERIALS
www.afm-journal.de

Development of a Multifunctional Platform Based on Strong, Intrinsically Photoluminescent and Antimicrobial Silica-Poly(citrates)-Based Hybrid Biodegradable Elastomers for Bone Regeneration

Yuzhang Du, Meng Yu, Juan Ge, Peter X. Ma, Xiaofeng Chen, and Bo Lei**

Biodegradable biomaterials with intrinsically multifunctional properties such as high strength, photoluminescent ability (bioimaging monitoring), and antimicrobial activity (anti-infection), as well as high osteoblastic differentiation ability, play a critical role in successful bone tissue regeneration. However, fabricating a biomaterial containing all these functions is still a challenge. Here, urethane cross-linked intrinsically multifunctional silica-poly(citrate) (CMSPC)-based hybrid elastomers are developed by first one-step polymerization and further chemical crosslinked using isocyanate. CMSPC hybrid elastomers demonstrate a high modulus of 976 ± 15 MPa, which is superior compared with most conventional poly(citrate)-based elastomers. Hybrid elastomers show strong and stable intrinsic photoluminescent ability (emission 400–600 nm) due to the incorporation of silica phase. All elastomers exhibit high inherent antibacterial properties against *Staphylococcus aureus*. In addition, CMSPC hybrid elastomers significantly enhance the proliferation and metabolic activity of osteoblasts (MC3T3-E1). CMSPC hybrid elastomers significantly promote the osteogenic differentiation of MC3T3-E1 by improving alkaline phosphatase activity and calcium biomineralization deposits, as well as expressions of osteoblastic genes. These hybrid elastomers also show a minimal inflammatory response indicated by subcutaneous transplantation in vivo. These optimized structure and multifunctional properties make this hybrid elastomer highly promising for bone tissue regeneration and antiinfection and bioimaging applications.

1. Introduction

Due to the trauma, disease, and population aging, the treatment and repair of large bone tissue loss and defects has become an urgent task for clinicians.[1] How to improve the efficiency and quality of bone tissue regeneration has been a major challenge for materials and biomedical scientists.[2] To solve these issues, the development of biomaterials with multifunctional properties instead of single function has been proposed for enhanced bone tissue regeneration.[3] Several functions, including biomimetic and high mechanical strength, osteoconductivity and osteoinduction, photoluminescent ability (bioimaging) and antibacterial properties (antiinfection), have demonstrated the positive effect on successful bone tissue regeneration.[4–6]

Most of human tissues including bone possess a typical viscoelastic mechanical behavior and relatively high mechanical strength.[7,8] Benefit from the elastomeric behavior, biomaterials can return to the original shape once the release of loading. This behavior of elastomeric materials

Y. Du, M. Yu, J. Ge, Prof. B. Lei
Frontier Institute of Science and Technology
Xi'an Jiaotong University
Xi'an 710054, China
E-mail: rayboo@xjtu.edu.cn
Prof. P. X. Ma
Department of Biologic and Materials Sciences
The University of Michigan
Ann Arbor, MI 48109-1078, USA
E-mail: mapx@umich.edu
Prof. P. X. Ma
Department of Biomedical Engineering
University of Michigan
Ann Arbor, MI 48109-1078, USA

DOI: 10.1002/adfm.201501712

Prof. P. X. Ma
Macromolecular Science and Engineering Center
University of Michigan
Ann Arbor, MI 48109-1078, USA
Prof. P. X. Ma
Department of Materials Science and Engineering
University of Michigan
Ann Arbor, MI 48109-1078, USA
Prof. X. Chen, Prof. B. Lei
National Engineering Research Center for Tissue Restoration and Reconstruction
Guangzhou 510006, China
Prof. B. Lei
State Key Laboratory for Manufacturing Systems Engineering
Xi'an 710054, China

makes them have high fatigue-resistant properties which is very helpful in the process of long term implanting. In addition, high mechanical strength such as elastic modulus is another feature of bone tissue. For example, trabecular bone and tibia possess an elastic modulus about 129 and 635 MPa, respectively.[9,10] Previous studies have shown that high elastic modulus can significantly enhance the osteoblasts attachment, proliferation and differentiation, thus improve the osteoproductivity.[11] Furthermore, bioceramics, such as bioactive silica-based glass and calcium phosphate, have exhibited the good osteoconductive ability.[12–14] Therefore, the incorporation of bioactive inorganic phase into polymer matrix can significantly improve the osteoconductive bioactivity.[15,16]

In recent years, biodegradable photoluminescent polymers have attracted much attention in tissue regeneration, bioimaging, and drug delivery.[17,18] As compared to photoluminescent quantum dots and organic dyes, intrinsically fluorescent biodegradable polymer possesses many unique advantages such as biodegradability, low toxicity, high photostability and quantum field, low photobleaching.[19] Moreover, in tissue regeneration, the degradation and movement of fluorescent polymer can be efficiently monitored and tracked, which is very favorable for successful tissue regeneration. However, few biodegradable polymer-based photoluminescent materials were developed for bone tissue repair and regeneration. Among the factors affecting tissue regeneration, bacterial infection after reconstruction surgery is an ever-present and serious complication.[20] To solve this issue, antibiotic drug administration and surgical debridement are the conventional treatments.[21] However, these methods usually resulted in some disadvantages such as the low efficiency, drug resistance, and additional surgery.[22] As a new alternative method, intrinsically antibacterial biomaterials possess many advantages such as high efficiency, continuous action, enhanced biocompatibility, and negligible drug resistance.[23] Ideal biomaterials for bone tissue regeneration and disease therapy should possess multifunction by combining osteostimulation, photoluminescence, antibacterial activity, and biomimetic mechanical behavior. To the best of our knowledge, few biomaterials possess intrinsically these functions ("all in one").

As one of poly(citrate)-based materials, synthetic biodegradable poly(1,8-octanediol-*co*-citrate) (PC)-based elastomers biomaterials has been extensively investigated due to their biomimetic viscoelastic properties, linear degradation profiles, and biocompatible degradation products.[24] These elastomers have been proposed for soft tissue applications, such as vascular graft and scaffold, myocardial biomaterials and so on, owing to its suitable mechanical and degradation properties.[25,26] Fluorescent PC elastomers have been developed through grafting amino acid on PC polymer.[27] However, low mechanical properties and poor osteogenic bioactivity limited their applications in bone tissue regeneration. On the other hand, silica-based bioactive materials possessed the good osteoconductivity and osteoproductivity and have become the promising candidate for bone tissue regeneration. Development of silica-poly(citrate)-based hybrid elastomers biomaterials perhaps can demonstrate new properties and may be a promising strategy for enhanced bone tissue regeneration.

In our previous work, silica grafted poly(1,8-octanediol-*co*-citrates) (SPOC) hybrid elastomers were successfully fabricated under high temperature and vacuum (thermal cross-linking) and they also showed general cellular biocompatibility including adipose-derived stem cells, fibroblast, myoblast, and osteoblasts.[28] However, the thermal crosslinked SPOC hybrid elastomers exhibited the poor strength (≈14 MPa) and elastomeric strain (≈134%) and stiffness (≈22 MPa), which is not suitable for bone tissue regeneration applications. On the other hand, chemical crosslinking strategy under low temperature has been shown as a highly effective method to improve the mechanical properties and multifunctionalities of bioelastomers.[17] Here, by a one-step polymerization and further isocyanate crosslinking method, we synthesized and characterized a novel biodegradable siloxane-grafted PC hybrid elastomer with "real" multifunctional properties (cross-linked intrinsically multifunctional silica-poly(citrate), CMSPC) including biomimetic mechanical strength, intrinsic photoluminescent, inherent antibacterial activity, and enhanced osteoblastic differentiation ability. We also investigated their osteoblasts biocompatibility including cell attachment, proliferation, osteogenic differentiation and inflammatory response in vivo. The development of novel hybrid elastomer may represent a new direction in multifunctional biodegradable biomaterials and have an important effect on tissue regeneration, tissue engineering and bioimaging.

2. Results and Discussions

2.1. Synthesis of MSPC Hybrid Prepolymers and CMSPC Hybrid Elastomers

By a one-step polymerization of citric acid, octanediol, and (3-aminopropyl) triethoxysilane (silane), multifunctional silica-based poly(citrate) hybrid (MSPC) prepolymers were prepared successfully under mild conditions without using any organic solvents, as shown in **Figure 1**a. The silane can be grafted on the side chain of prepolymer by the chemical reaction between amino and carboxyl group of citric acid (Figure 1b). In this procedure, the hydrolysis of silane and Si—OH may occur because of the presence of water after polycondensation. The prepolymers were further crosslinked into multifunctional silica-based poly(citrate) hybrid elastomers (CMSPC) by 1,6-hexamethyl diisocyanate (Figure 1b). In the chemical crosslinking, the hybrid polymer networks were formed and inorganic Si—O—Si structure was hybridized into polymer matrix successfully (Figure 1c). The structure, physicochemical properties, and biocompatibility can be highly tunable by controlling the inorganic phase contents, HDI concentration, and curing temperature.

2.2. Structure Characterization of Hybrid Prepolymers and Elastomers

The chemical structure and successful synthesis of MSPC hybrid prepolymer and CMSPC elastomers were indicated by ^{1}H NMR, FTIR spectroscopy, and GPC test. As shown in the ^{1}H NMR spectroscopy of PC and MSPC hybrid prepolymers, the representative methylene peaks (—C$\underline{H_2}$—) identified at 1.27, 1.54, and 3.97 ppm and between 2.64 and 2.89 ppm

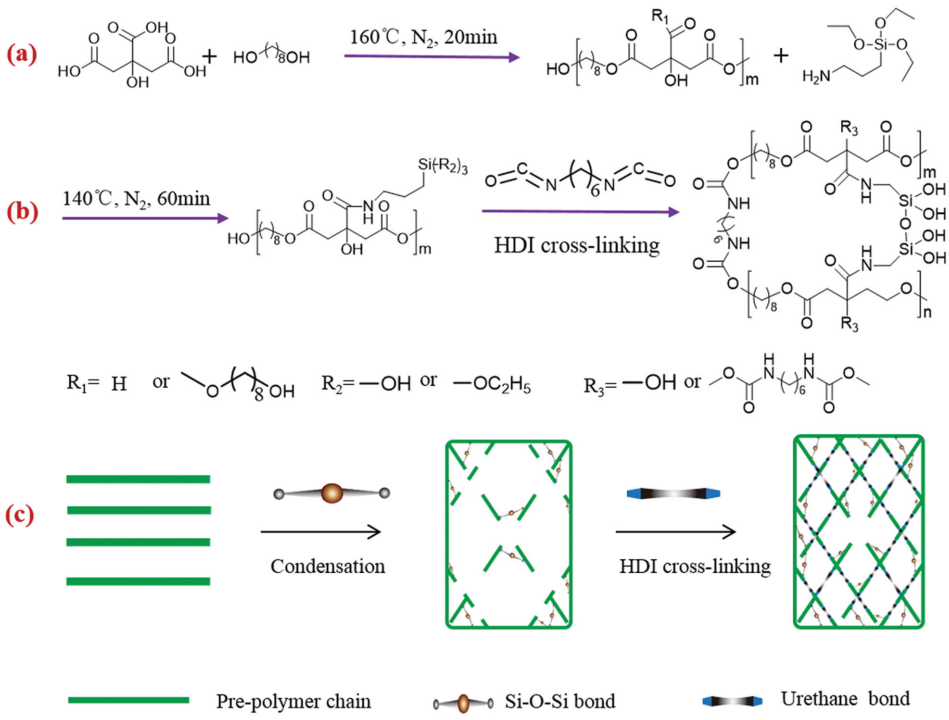

Figure 1. Synthesis of multifunctional silica-poly(citrate)-based hybrid prepolymers and elastomers. a,b) Fabrication of MSPC and CMSPC elastomers by polycondensation of CA, OD, AS, as well as the chemical crosslinking with HDI and c) schematic diagram showing the formation of CMSPC hybrid elastomers matrix.

(—CH_2—) were attributed to 1,8-octanediol and citric acid, respectively (Figure S1a, Supporting Information). For MSPC prepolymer, the presence of characteristic peaks at 7.59 ppm (—NH—) from AS confirmed the successful grafting of silane on the side chain of PC polymer (Figure S1b, Supporting Information). The average molecular weight of as-prepared MSPC prepolymers showed a significant increase from 5004 to 28 726 g mol^{-1} as the increase of silica phase contents, compared to pure PC prepolymer (Table S1, Supporting Information). In addition, all prepolymers possessed a polydispersity below 1.2, indicating the narrow molecular distributions.

The chemical structure of MSPC prepolymers and hybrid elastomers was further identified by FTIR, as shown in **Figure 2**a,b. The unreacted hydroxyl (—OH) groups in PC and MSPC structure were found at 3200–3600 cm^{-1}. The ester bonds (—C=O) formation of prepolymers was identified by the presence of characteristic peaks at 1720–1740 cm^{-1}. The double peaks between 2800 and 3000 cm^{-1} were attributed to the methylene (—CH_2—) from diols. The characteristic bands at 1100–1200 cm^{-1} were assigned to the C—N stretching vibration, which confirmed the successful grafting of silica into PC. For the FTIR of elastomers, the significant decrease of hydroxyls, disappearance of C=N at 2300–2500 cm^{-1}, the presence of —NH (3200–3400 cm^{-1}) and amide (1550–1650 cm^{-1}) confirmed the successful chemical crosslinking by HDI (**Figure 3**a,b). Moreover, the significantly enhanced bands at 1000–1100 cm^{-1}

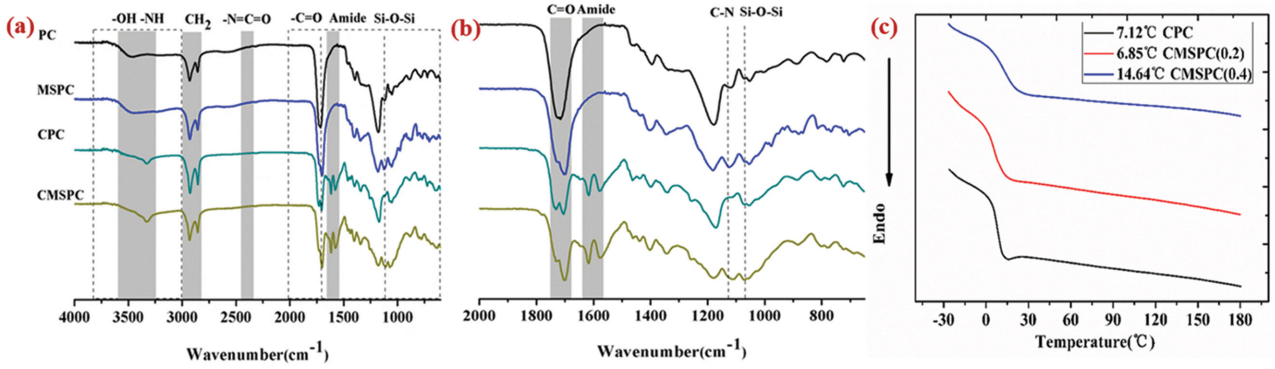

Figure 2. Chemical structure and thermal stability of MSPC prepolymer and CMSPC hybrid elastomers. a,b) FTIR spectra between a) 4000–650 cm^{-1} and b) 2000–650 cm^{-1}, indicating the formation of polyester and silica hybrid structures; c) DSC curves showing the low glass transition temperature (T_g) below room temperature of CPC and CMSPC elastomers.

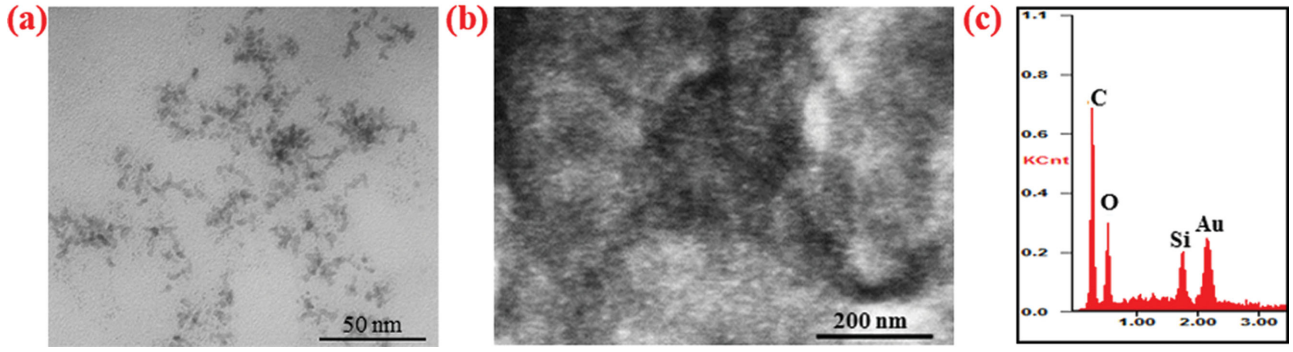

Figure 3. Microstructure and nanostructure of CMSPC hybrid elastomers. a) TEM image demonstrating the nanostructure of hybrids; b) SEM image presenting the microstructure of hybrids; and c) EDS spectrum showing the elemental composition.

identified as Si—O—Si confirmed the formation of silica networks.[29] The ^{1}H NMR and FTIR spectroscopies demonstrated that MSPC and CMSPC hybrid elastomers were successfully synthesized.

Inorganic phase incorporation into polymer elastomers matrix may have an important effect on thermal properties. Here DSC and TG analyses were used to evaluate the glass transition temperature (T_g) and thermal stability (Figure 2c). Due to the addition of silica phase, CMSPC showed a significantly enhanced T_g (6.8 °C and 14.6 °C) compared to that of CPC elastomer (7.1 °C). No any obvious crystallization peaks were observed for all elastomers. The low T_g below room and body temperatures suggested the highly elastomeric mechanical behavior of our CMSPC hybrids when in vivo applications. These results demonstrated that the silica phase doping significantly enhanced the thermal properties of CPC elastomers. The polymer T_g was usually determined by the chains mobility and low mobility may result in the high T_g. Compared to CPC, both thermal crosslinked and Si—O—Si hybrid network presented in CMSPC hybrid elastomers, which would limit the chains mobility. In addition, the strong hydrogens bonding interactions between —NH— groups may also contribute to the improvement of the thermal properties for CMSPC hybrids. The microstructure and nanostructure and composition of CMSPC elastomers were also evaluated by SEM and TEM analysis, as shown in Figure 3. The TEM images of ultra-thin section of samples clearly showed the uniform distribution of silica phase (5–10 nm) in polymer matrix (Figure 3a). The nanoscale distribution of inorganic phase was also confirmed from SEM image and EDS analysis demonstrated the presence of Si in hybrid structure (Figure 3b,c).

The results shown above, including ^{1}HNMR, GPC, FTIR, clearly indicated that the MSPC and CMSPC hybrid polymer was synthesized successfully through one-step polymerization of citric acid, diols, and silane. TEM and SEM images showed the representative microstructure and uniform nanostructure of organic–inorganic hybrid elastomers. The DSC result demonstrated the elastomeric behavior of CMSPC hybrids at body temperature. Based on the advantages of bioactive silica-based materials, the inorganic phase incorporation may produce a critical effect on physicochemical properties and biocompatibility of PC-based elastomers.

2.3. Strong Mechanical Behavior of CMSPC Hybrid Elastomers

Human hard tissues, including bone, cartilage, and tendon, possess high mechanical strength and modulus. Artificial biomaterials should have enough mechanical properties to match the repair and regeneration of these tissues. Conventional biodegradable polymer elastomers such as poly(citrate) and poly(glycerol) cannot meet these requirements, due to their low strength and modulus.[30] There is still much need to develop new biodegradable elastomers with high mechanical properties. In this study, inorganic silica phase was covalently grafted into PC matrix to tailor their mechanical properties, as shown in **Figures 4** and **5**, and **Table 1**. Our CMSPC hybrids showed fast recovery after bending and stretching, indicating their highly elastomeric behavior (Figure 4a–c). The typical viscoelastic stress–strain behavior for CMSPC hybrid elastomers was also observed (Figure 4d). When DMF was used as the solvent, the tensile strength, elongation, and modulus of synthesized hybrid elastomers could be controlled in the range from 1.29 ± 0.25 to 9.61 ± 0.33 MPa, 200% ± 48% to 346% ± 12%, and 4.21 ± 0.27 to 44.23 ± 2.9 MPa, respectively (Figure 4e–g and Table 1). These results demonstrated that seven times and ten times improvement for tensile strength and modulus could be received by incorporating silica phase, as compared to pure PC elastomers. Further study showed that the similar stress–strain behaviors for CPC and CMSPC elastomers after third cycle test were observed, indicating their good antifatigue ability and highly elastomeric behavior (Figure S2, Supporting Information).

However, when dimethyl sulfoxide was employed as the solvent, as-prepared elastomers showed very different mechanical behavior especially for the elastic modulus, as shown in Figure 5. All samples showed the representative viscoelastic stress–strain behavior in the range of 10% strain, although the plastic deformation happened after further stretching (Figure 5a–c). The ultimate tensile strength was significantly improved with the increase of silica ratio and crosslinking temperature and controlled by HDI content (Figure 5a–c,f). By optimizing various parameters, the final Young's modulus, tensile stress, and elongation at break of CMSPC hybrid elastomers could highly tuned from 44.12 ± 13.54 to 976.93 ± 15.86, 3.59 ± 0.42 to 25.0 ± 3.49 MPa, 14% ± 4% to

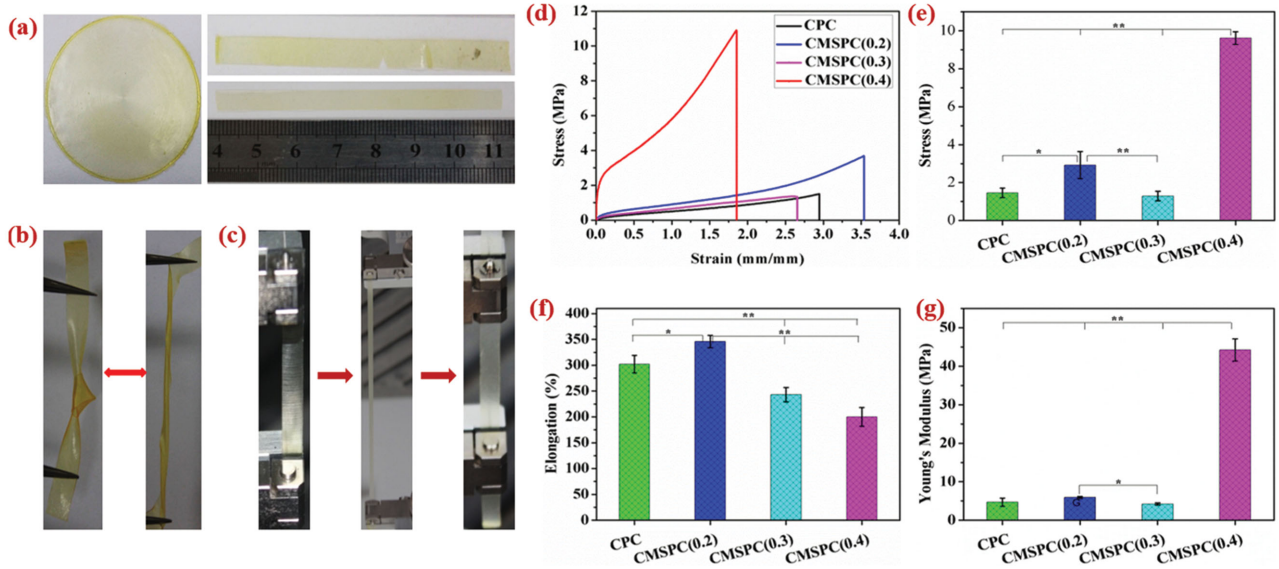

Figure 4. Highly tunable mechanical properties of CMSPC hybrid elastomers as change with silica phase contents. a) Optical photos of hybrid elastomers; b,c) highly tough and elastomeric characteristic; d–g) highly elastomeric d) stress–strain behavior, e) tensile strength, f) elongation, and g) tensile modulus of CPC and CMSPC hybrid elastomers. The incorporation of silica phase significantly enhanced the tensile stress and modulus, as well as keeping comparable elongation, compared with CPC elastomers. (*$P < 0.05$, **$P < 0.01$, $n = 5$).

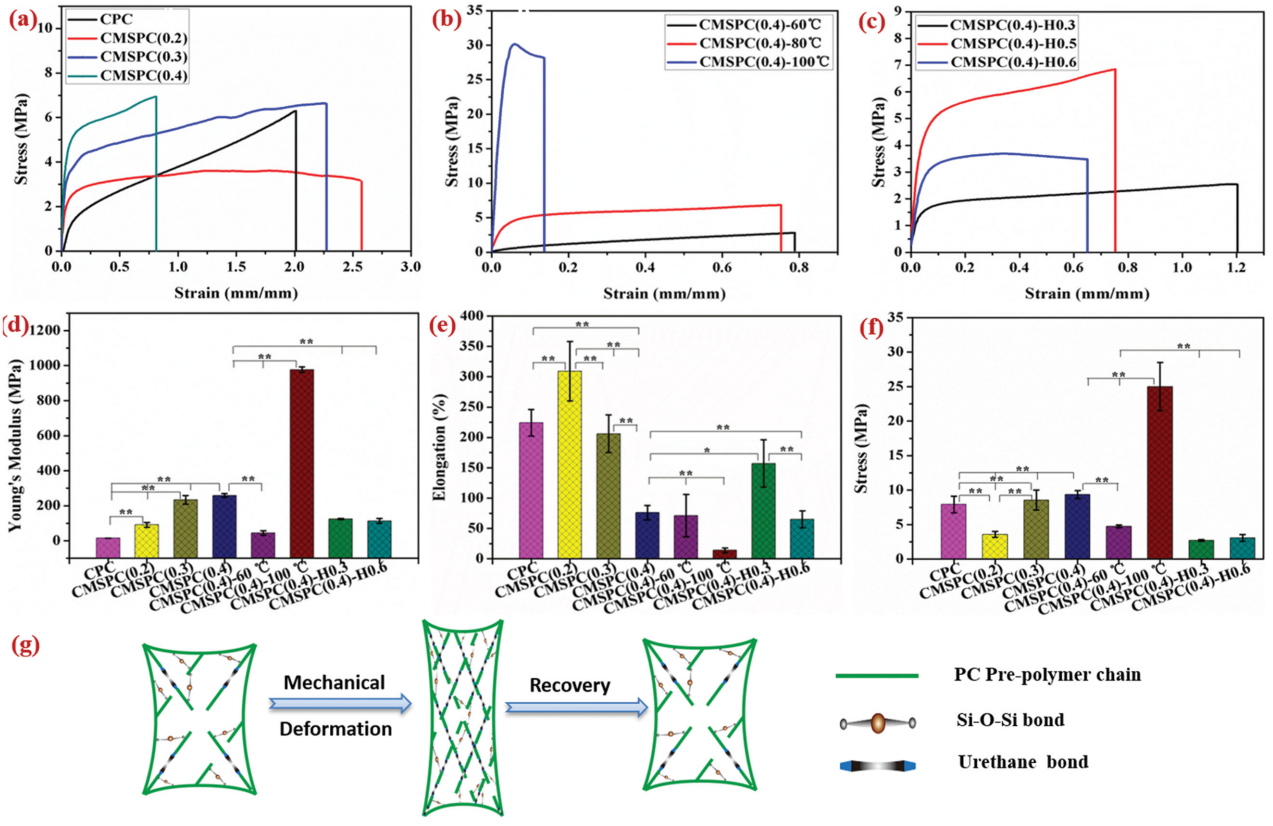

Figure 5. Highly tunable mechanical properties of CMSPC hybrid elastomers as change with solvents, chemical crosslinking temperatures, and molar ration of HDI. a–c) Highly elastomeric stress–strain behaviors of samples dissolved in DMSO after curing at 80 °C a), under different crosslinking temperature b) and various HDI concentration c); d,e) tensile stress, elongation, and tensile modulus of all hybrid elastomers; f) schematic diagram of high mechanical properties of CMSPC hybrid elastomers; and g) mechanical deformation and recovery process of CMSPC hybrids (*$P < 0.05$, **$P < 0.01$).

Table 1. Highly tunable mechanical properties of elastomeric CMSPC hybrids.

Samples	Ultimate tensile stress [MPa]	Elongation [%]	Young's modulus [MPa]
CPC (DMF)	1.46 ± 0.25	302 ± 17	4.68 ± 1.07
CMSPC(0.2) (DMF)	2.92 ± 0.71	346 ± 12	5.92 ± 0.27
CMSPC(0.3) (DMF)	1.29 ± 0.25	243 ± 34	4.21 ± 0.27
CMSPC(0.4) (DMF)	9.61 ± 0.33	200 ± 48	44.23 ± 2.9
CPC (DMSO)	7.92 ± 1.2	224 ± 22	14.78 ± 0.61
CMSPC(0.2) (DMSO)	3.59 ± 0.42	309 ± 49	91.14 ± 14.3
CMSPC(0.3) (DMSO)	8.56 ± 1.45	206 ± 31	233.18 ± 24.65
CMSPC(0.4) (DMSO)	9.36 ± 0.56	76 ± 12	258.63 ± 10.78
CMSPC(0.4)-60 °C (DMSO)	4.75 ± 0.21	71 ± 35	44.12 ± 13.54
CMSPC(0.4)-100 °C (DMSO)	25.0 ± 3.49	14 ± 4	976.93 ± 15.86
CMSPC(0.4)-H0.3(DMSO)	2.7 ± 0.13	157 ± 39	124.3 ± 3.85
CMSPC(0.4)-H0.6(DMSO)	3.08 ± 0.5	65 ± 14	113.28 ± 13.9

309% ± 49%, respectively (Figure 5d–f and Table 1). Moreover, compared with the thermal crosslinked SPOC hybrid elastomers, the Young's modulus, elongation at break, and tensile stress of CMSPC hybrid elastomers showed the improvement of 44 times, 3 times, and 2 times, respectively. These results further demonstrated the advantages of chemical crosslinking on improving mechanical p roperties of bioelastomers. As compared to the stress–strain curves of SPOC elastomers, our CMSPC hybrid elastomers exhibited the representative stress yield at the last stage of strain (Figures 4 and 5). Even so, CMSPC still showed highly elastomeric behavior in the range of 30% strain (similar with native bone tissue) which may be associated with their composition and structure. Compared with thermal crosslinked SPOC elastomers, isocyanate (HDI) crosslinking could significantly increase the polymer chain mobility and content of hard segments. Thus, CMSPC showed significantly higher elastomeric strain and modulus than those of thermal crosslinked SPOC elastomers. Our results were also consistent with the previous report about HDI cross-linked bioelastomers.[17]

As compared to pure CPC elastomers, the significant improvement of mechanical properties as the increase of silica content could be attributed to the high stiffness of inorganic silica networks (Si—O—Si) and molecular-level distribution in polymer matrix. This result was in accordance with previous reports on silica-based polymer hybrid biomaterials.[31–33] The increase of cross-linking temperature and HDI content significantly enhanced the mechanical strength, which was probably due to the increase of cross-linked density (limiting the movement of polymer chain) (Figure 5). However, too high HDI content would decrease greatly the polymer chain movement, increase the brittleness and then reduce mechanical properties. On the other hand, the mechanical properties of our hybrid elastomers especially the elastic modulus seemed as very different when prepolymers were dissolved in different solvents including DMF and DMSO. Almost 10 times improvement in elastic modulus for our hybrid elastomers was obtained when preparing in DMSO compared to that in DMF. This difference may be explained from the cross-linking density and molecular interactions in polymer hybrid matrix. Generally, the elastic modulus of materials is depending on the bonding intensity between molecules or atoms. In our study, in comparison with DMF, DMSO possesses a high polarity. Therefore, the MSPC hybrid prepolymer may have high solubility and chain stretching in DMSO, which would increase the crosslinking points and crosslinked density. The increase of crosslinking degree would enhance the bonding intensity between polymer chains and improve the elastic modulus.

Human hard tissues including bone, teeth, and tendon possess high mechanical strength especially the elastic modulus, as well as remaining high viscoelastic behavior. Conventional biodegradable elastomers such as PC and poly(glycerol sebacate) (PGS) polymers usually showed low stiffness and narrow mechanical range. The CMSPC-based hybrid elastomers we developed here presented highly tunable mechanical properties (44–976 MPa in modulus, 3–25 MPa in tensile strength, and 14%–309% in strain) which were much higher than those of most soft tissues and comparable to human bone tissues such as trabecular bone (≈129 MPa in modulus) and tibia tissues (≈635 MPa in modulus).[34,35] These excellent mechanical properties make our CMSPC-based hybrid elastomers promising in hard tissue regeneration applications.

2.4. In Vitro Hydrophilicity and Degradation Behavior of CMSPC Hybrid Elastomers

The controlled hydration ability and degradability for biomaterials was very important and may determine their suitable applications in tissue regeneration. Here we examined the effect of silica phase incorporation on the hydrophilicity and degradation, as shown in **Figure 6**a,b. Pure CPC elastomers presented a water contact angle of 79° ± 3° (0 min) (Figure 6a). The water contact angle for CMSPC hybrid elastomers significantly decreased to be 60° ± 2° (CMSPC 0.4) and changed to be 52° ± 2° after 2 min, indicating their enhanced hydrophilicity feature. The improved hydrophilicity for CMSPC could be attributed to the hydrophilic character of Si—O—Si network. The in vitro biodegradation was also carried out by soaking samples in NaOH solution (0.01 M) at 37 °C (Figure 6b). The biodegradation method in alkaline solution for evaluating the PC-based elastomers has been well used in previous reports.[36] High HDI content could significantly decrease the degradation rate. No significant difference in alkaline degradation between CPC and CMSPC elastomers was observed over periods of 5 h. This result could be explained by the chemical structure and hydrophilicity of elastomers. The addition of silica phase increased the polymer crosslinked density and may enhance the water-resistant ability. On another hand, Si—O—Si networks also improved the hydrophilicity of hybrid elastomers which may cause the high water uptake and alkaline degradation. That was why no significant difference in degradation between CPC and CMSPC was obtained. It should be noted that the in vitro degradation rate of CMSPC would be slow if the medium was PBS. Actually, in previous study, we have tested the in vitro degradation in PBS for thermal crosslinked SPOC hybrid

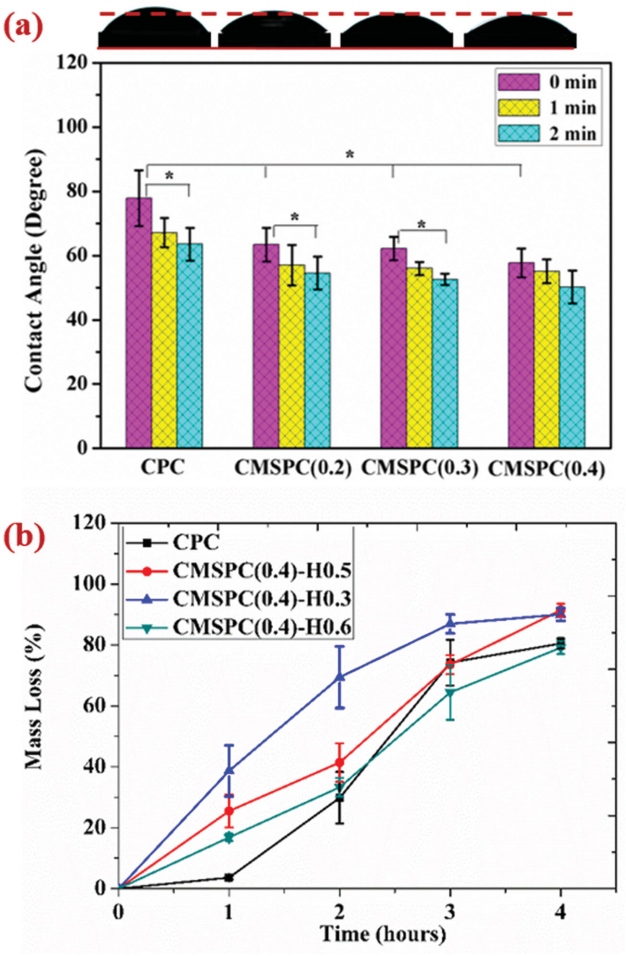

Figure 6. Hydrophilicity and biodegradation evaluation of CMSPC hybrid elastomers. a) Water contact angle test as the change of time; b) weight loss after incubation in 0.01 M NaOH (*$P < 0.05$, $n = 5$). CMSPC hybrid elastomers showed significantly enhanced hydrophilicity and controlled biodegradation ability.

elastomers and the results showed that only 23% weight loss was observed after 30 d soaking.[28] Therefore, we believe that our CMSPC should have the similar degradation behavior and relatively stable mechanical properties in vivo applications.

2.5. Inherent Antibacterial Properties of CMSPC Hybrid Elastomers

In the process of the biomaterials applications in vivo, implants infections have become the significant complication, affected the implant success and accounted for high medical cost. To show the potential antiinfection properties, the antibacterial ability of our CMSPC hybrid elastomers was evaluated. **Figure 7** shows the effect of hybrid elastomers on the activity of common *Staphylococcus aureus*. When culture with CPC and CMSPC elastomers, *S. aureus* activity significantly decreased as the increase of incubation time (Figure 7a). Almost 100% killing ratio of *S. aureus* could be obtained after 24 h incubation with samples (Figure 7b). Actually the *S. aureus* growth has disappeared only 16 h incubation with materials (Figure 7c). The high antibacterial activity may be attributed to the acidic chemicals-releasing property of CPC and CMSPC elastomers after soaking in buffer solution medium.

To explore the antibacterial mechanism, we investigated the pH change of PBS after soaking CPC and CMSPC films into PBS for different time under static and dynamic conditions (Figure S3, Supporting Information). The pH value significantly decreased as increasing soaking time (pH < 6 after 24 h), when the PBS was not refreshed (static condition), as indicated in Figure S3a (Supporting Information). However, under the dynamic condition (refreshing PBS every day), the pH value rapidly returned to the normal value (pH 7.2) after 3 d soaking (Figure S3b, Supporting Information). CMSPC hybrid elastomers demonstrated the significantly high pH buffer capacity either the static or dynamic conditions, as compared to CPC elastomers. The pH difference after soaking for CPC and CMSPC could be ascribed to the chemical structure and degradation products. In our study, PC was synthesized by polymerizing citric acid and octanediol. After reaction, the carboxylic acid remained in the structure of prepolymer may cause the acidic feature of CPC elastomers. In addition, previous reports have shown that the acid and diol were mainly the degradation byproducts of PC-based elastomers.[27] These factors should be responsible for the pH decrease of CPC. The addition of silica phase consumed most of carboxyl groups in polymer, which would significantly suppress the acidic carboxyls residual in CMSPC structure. It should be noted that the low pH (below 6.5) of elastomers-incubated medium at the early period of soaking may be responsible for the antibacterial activity. Because the implants infection usually happened at the started period of transplantation, our hybrid elastomers could exactly provide the antibacterial ability in this stage.

2.6. Intrinsical Photoluminescent Properties of CMSPC Hybrid Elastomers

The intrinsical photoluminescent ability of our hybrid elastomers was also studied due to the increasing interest on degradable fluorescent materials for biomedical applications. Without adding any fluorescent dye or quantum dots in polymer matrix, our MSPC prepolymer and CMSPC hybrid elastomers demonstrated significantly strong photoluminescent ability (**Figure 8**). The strong blue-emission fluorescence could be observed from MSPC prepolymer solution (Figure 8a) and CMSPC elastomers films (Figure 8b). Under excitation at 360 nm, compared to PC, the significantly increased fluorescent emission for MSPC was observed (Figure 8c). In addition, as excitation wavelength (from 360 to 430 nm) increased, the emission position of MSPC was significantly moved to high wavelength (from 400 to 550 nm). It is well known that conjugated polymer systems possess highly fluorescent emissions ability.[37] However, in the structure of MSPC hybrid polymer, no any obvious conjugated groups were observed, indicating that conjugated mechanism is not the reason of photoluminescent properties. In addition to the conjugated mechanism, the structure defect and impurities were usually

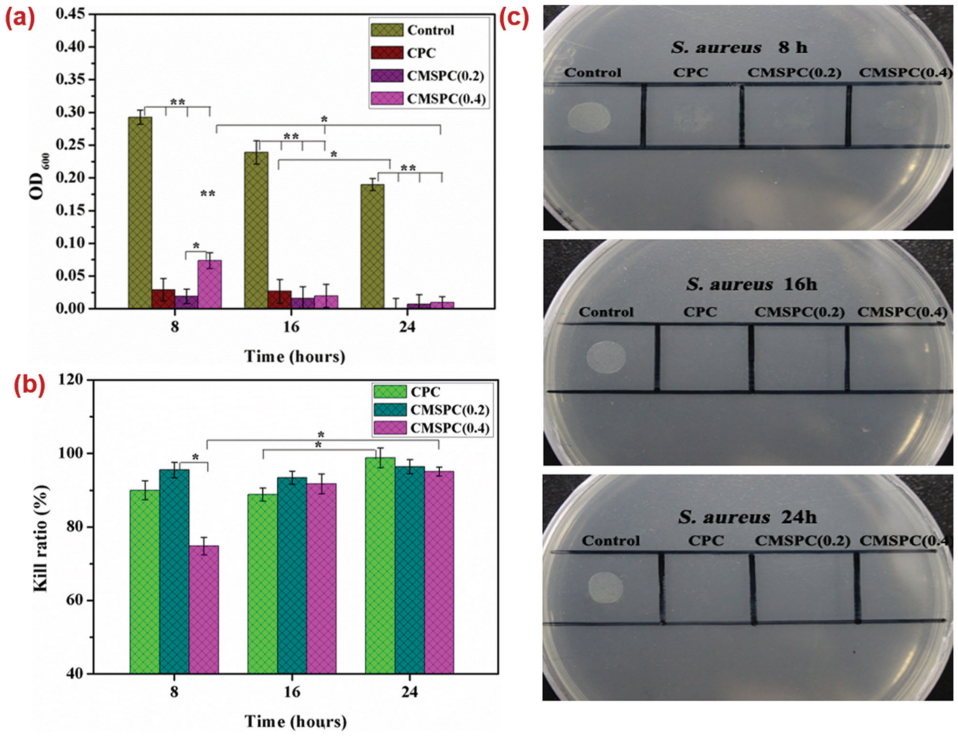

Figure 7. Inherent antibacterial activity investigation of CMSPC hybrid elastomers. a) *S. aureus* activity after incubation with elastomers for different times; b) *S. aureus* killing ratio after incubation; c) growth inhibition of bacteria (*S. aureus*) on agar plate for incubation time of 8, 16, and 24 h. (*$P < 0.05$, **$P < 0.01$, $n = 5$). Significantly high antibacterial ability could be observed for CPC and CMSPC elastomers.

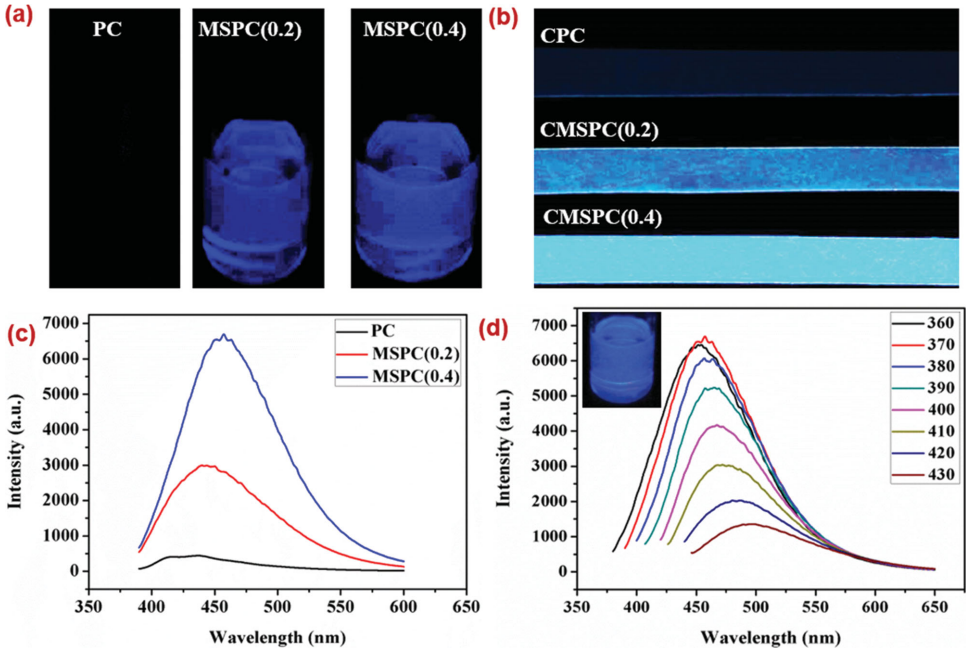

Figure 8. Intrinsical photoluminescent properties evaluation of and MSPC and CMSPC hybrids. a) Blue fluorescence emission of MSPC prepolymer solution at a concentration of 1 mg mL^{-1} excited by UV at 365 nm; b) fluorescent images of CMSPC elastomers excited by UV at 365 nm; c) fluorescent emission spectra of MSPC hybrids under excitation at 360 nm; and d) fluorescent emission spectra of MSPC (0.4) hybrids under different excitation wavelengths. MSPC and CMSPC hybrids showed significantly enhanced photoluminescent ability as compared with PC and CPC polymers.

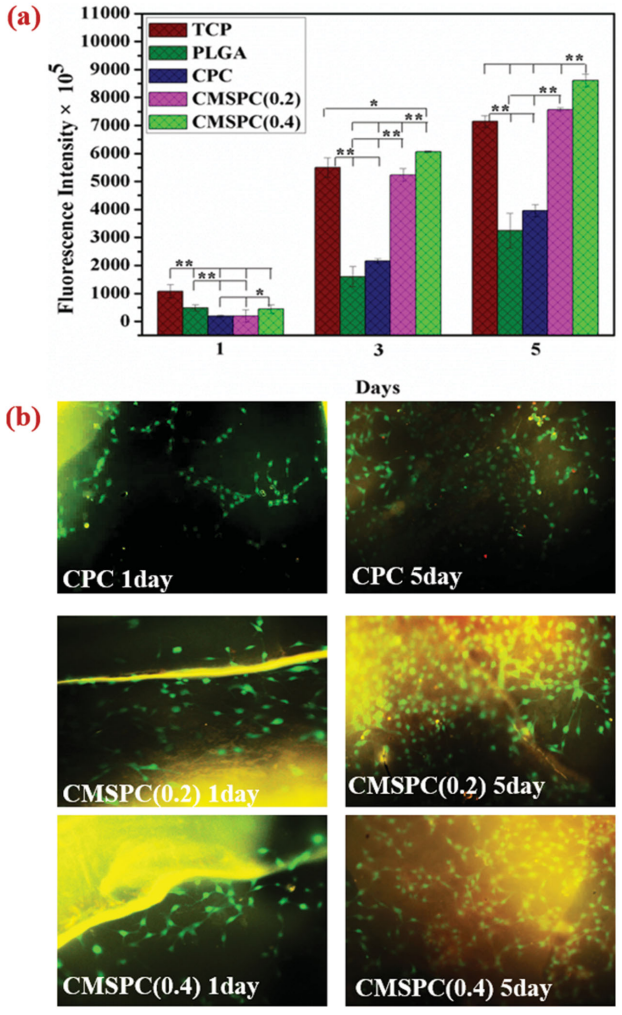

Figure 9. Osteoblast cells biocompatiblity assessment after culture on CMSPC hybrid elastomers. a,b) MC3T3-E1 cells proliferation a) and fluorescent images (b, 10× microscopy) after incubation for 1, 3, and 5 d, indicating the significantly enhanced cell growth and metabolic activity induced by CMSPC hybrid elastomers, PLGA and CPC was used as controls. (*$P < 0.05$, **$P < 0.01$, $n = 5$).

considered as the possible mechanism for explaining the photoluminescent properties of silica-based materials.[38] In our study, the MSPC polymer was synthesized under high temperature and vacuum and carboxylic acid monomers may be remained in the structure of polymer. In this process, carbon substitutional defect center for Si could be formed due to the decomposition of carboxylate, which induced the photoluminescent ability of MSPC and CMSPC hybrids.

2.7. High Osteoblasts Biocompatibility of CMSPC Hybrid Elastomers

To evaluate the practicability of CMSPC hybrid elastomers for bone tissue regeneration applications, osteoblast cells (MC3T3-E1) were used to determine the cellular biocompatibility of materials. **Figure 9** exhibits MC3T3-E1 cells morphology, proliferation, and metabolic activity after culture for 1–5 d on surfaces of CPC and CMSPC hybrid elastomers. Cells showed a significant growth on all materials as the increase of culture time (Figure 9a). At 3 and 5 d, the cells activities on CMSPC hybrid elastomers were significantly higher than those on CPC and PLGA and TCP controls, suggesting the enhanced cell proliferation ability of CMSPC. The fluorescent images also presented the much cell spreading morphology at 1 and 5 d on surfaces of CMSPC, in comparison with CPC elastomers (Figure 9b). In addition, the cell metabolic activity was significantly enhanced by the increase of silica grafting contents.

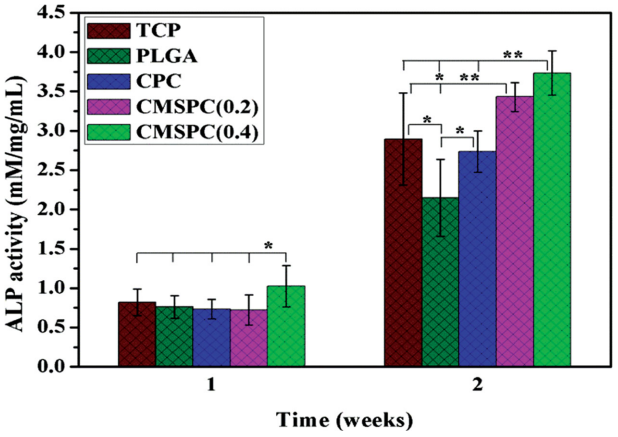

Figure 10. ALP activity evaluation showing the osteogenic differentiation of MC3T3-E1 cells after culture for 1 and 2 weeks. Osteoblasts demonstrated significangtly enhanced ALP activity when culturing on CMSPC hybrid elastomers as compared with CPC and PLGA controls. *$P < 0.05$ and **$P < 0.01$ represented the significant difference between various groups ($n = 5$).

2.8. Improved ALP Activity and Biomineralization by CMSPC Hybrid Elastomers

To further demonstrate the potential in application for bone regeneration, the osteogenic differentiation of cells after culture with CMSPC hybrid elastomers was investigated using pure CPC elastomer and commercial PLGA as controls. **Figure 10** shows the ALP activity of cells after incubation with CMSPC hybrid elastomers for 1 and 2 week. The ALP activity for all samples significantly increased as improved culture periods up to 2 weeks. At both 1 and 2 weeks, cells on CMSPC hybrid elastomers demonstrated significantly high ALP activity compared with CPC and PLGA film, as well TCP control. In addition, cells on CMSPC (0.4) presented significantly enhanced ALP activity in comparison with CMSPC (0.2) hybrid elastomers, indicating that Si incorporation significantly improved the ALP activity and early differentiation of osteoblasts.

The cellular biomineralization after culture for 2 weeks was confirmed by von Kossa staining, as shown in **Figure 11**. Histology with von Kossa staining revealed that there was heavy mineral deposition (black brown) on the surface of CMSPC

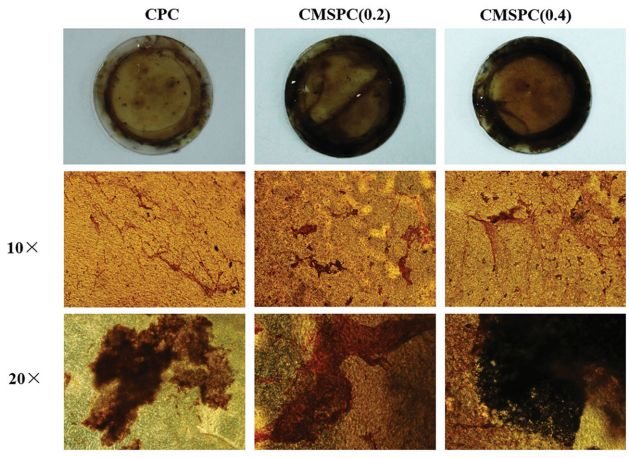

Figure 11. Osteogenic differentiation evaluation of MC3T3-E1 cells after culture with as-prepared elastomers. Calcium deposition analysis stained by Von Kossa kit after culturing cells for 2 weeks, suggested the significantly improved calcium deposition on CMSPC hybrids.

hybrid elastomers, while there was little observable mineralization on CPC control. In addition, the heavy deposition was significantly improved as increasing silica doping concentration. It should be noted that the mineral deposition was not detected on hybrid elastomers without seeding cells (data not shown), suggesting the enhanced ability of hybrid elastomers for cellular biomineralization.

2.9. Genes Expression of Osteoblastic Differentiation Markers

The enhanced osteoblastic differentiation of cells was further determined by investigating the gene and proteins expressions levels after culture with materials for different time periods. **Figure 12** shows the expression profiles of ALP, OCN, OPN, and RUNX-2 from cells after incubation with PLGA, CPC, and CMSPC hybrid elastomers for 1, 2, and 3 weeks. Here, TCP, PLGA, and CPC were used as controls. At 1 week, the gene expression of ALP, OPN, and RUNX2 from cells cultured on CMSPC (0.2) hybrid elastomers was significantly higher compared to those on TCP, PLGA, and CPC controls ($p < 0.05$). After culture for 2 weeks, mRNA levels of ALP, OCN, OPN, and RUNX2 in cells on CMSPC (0.4) were significantly enhanced as compared with TCP, PLGA, CPC controls, and CMSPC (0.2) hybrid elastomers ($P < 0.01$). At 3 weeks, the ALP and RUNX2 genes from cells on CMSPC (0.4) still demonstrated significantly higher expressions levels than all other groups. It should be noted that the osteogenic genes expressions (ALP, OCN, OPN, and RUNX2) of cells incubated with elastomers groups for 3 weeks (CPC and CMSPC) were significantly high compared to commercial PLGA biomaterial group, which suggested that elastomeric biomaterials may be favor of improving osteoblastic gene expression. In the whole culture periods, CMSPC hybrids could significantly upregulate the osteoblastic genes expressions compared with CPC and PLGA groups. This result was also consisted with that of ALP activity analysis after 2 weeks incubation (Figure 11).

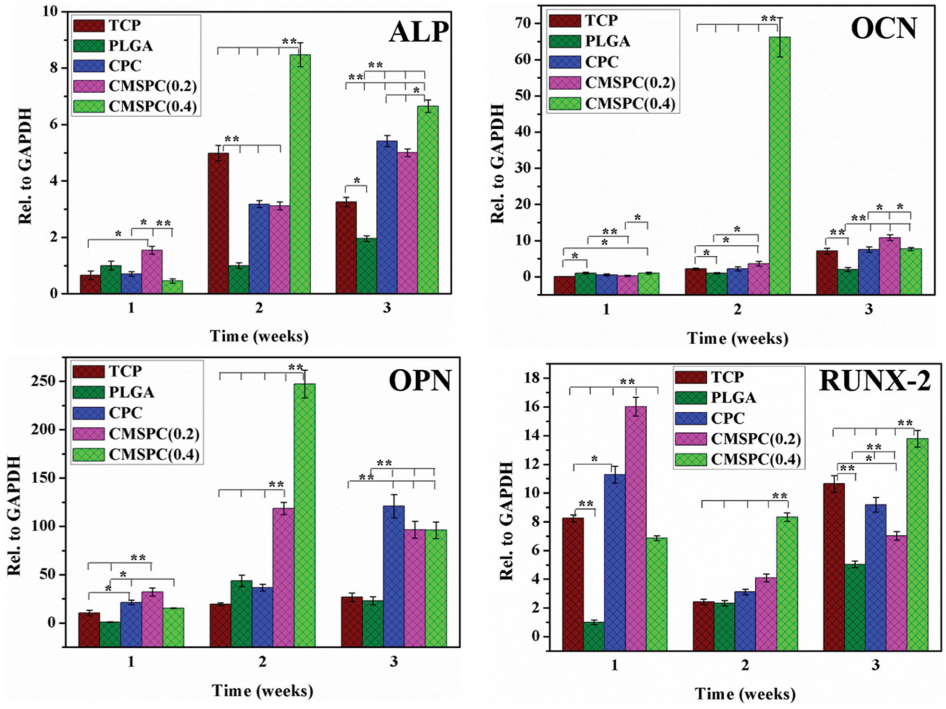

Figure 12. Osteoblastic genes expressions profiles of cells cultured on CMSPC hybrid elastomers. ALP, OCN, OPN, and RUNX-2 expressions levels of MC3T3-E1 cells after incubation with CMSPC hybrid elastomers for 1, 2, and 3 weeks, PLGA and CPC were used as controls. Significant differences were considered when $*P < 0.05$ and $**P < 0.01$ ($n = 5$). Significantly upregulated osteoblastic genes levels were observed for CMSPC hybrid elastomers as compared with CPC and PLGA controls.

Although biodegradable polymer elastomers have been developed and applied in soft tissue regeneration and have achieved many results in enhancing the biocompatibility of soft tissues-related cell types, the effect of polymer elastomers on osteoblastic differentiation was never reported. Here we first fabricated chemical crosslinked silica-based PC bioelastomers and studied the influence of hybrids on osteoblastic differentiation. CMSPC elastomers demonstrated the significantly enhanced ability for osteoblastic differentiation, compared with PLGA and CPC controls. Silicon is a very important trace element for mediating the bone tissue formation and metabolism.[38] Previous reports have proved that silica-based biomaterials including bioactive glasses and silicate ceramics could significantly promote the differentiation of osteoblasts and bone formation.[39,40] Further studies also indicated that silica-based biomaterials could efficiently activate the osteogenic genes expressions through eukaryotic protein kinases (EPK) and mitogen-activated protein kinase (MAPK) pathways.[41,42] In our study, CPC elastomers also showed high ability enhancing ALP activity and osteogenic gene expressions of osteoblasts, as compared to commercial PLGA film, which suggested that elastomeric polymer may be suitable to be as good candidate for bone repair and regeneration. After incorporating silica phase into elastomeric matrix, significantly high osteogenic differentiation ability of CMSPC hybrids was observed. The multifunctional properties including strong mechanical behavior and intrinsic photoluminescence and inherent antimicrobial ability, as well as high osteoblastic activity, make our CMSPC hybrid elastomers promising applications for bone tissue regeneration and drug delivery.

2.10. In Vivo Inflammatory Response

The in vivo biocompatibility of CMSPC hybrid elastomers was evaluated in a rat model by subcutaneous dorsal implantation followed by H&E staining after 2 or 4 weeks. As shown in **Figure 13**, all CMSPC hybrid elastomers demonstrated decreased fibrous capsule formation when compared to pure CPC elastomers, indicating their low inflammation responses. The fibrous capsule thickness of SPOC hybrid elastomers was significantly lower compared to the PLGA implants (FDA-approved polymer), which showed a thickness of 150 and 1000 μm for implantation of 1 and 12 weeks, respectively.[43] Therefore, consistent with in vitro observations, our CMSPC hybrid elastomers showed decent biocompatibility in vivo. However, more detailed in vivo studies on biological responses and tissue regeneration are required to further evaluate the application potential of our CMSPC hybrid elastomers.

3. Conclusion

In summary, CMSPC hybrid elastomers can be facily synthesized through thermal polymerization and chemial crosslinking process under mild conditions. CMSPC-based hybrids demonstrate highly tunbale mechanical properties that are compliant with strong biological tissues such as bone and cartilage and tendon. The biodegradation rate of CMSPC elastomers can be tarilored by the degree of crosslinking. In addition, our MSPC and CMSPC hybrids exhibit strong intrinsical photoluminescence with broad ranges of emissions. The inherent high antibacterial activity against *S. aureus* was also observed from CPC and CMSPC elastomers. CMSPC derivatives can significantly enhance osteoblasts attachment, proliferation, and differentiation activity through activating osteoblastic genes expressions, while exhibiting low inflammation response in vivo. It can be envisaged that the CMSPC hybrids may serve as a multifunctional platform including photoluminescence and antibacterial and osteoproductivity abilities for highly bone tissue regeneration and bioimaging and antiinfection applications.

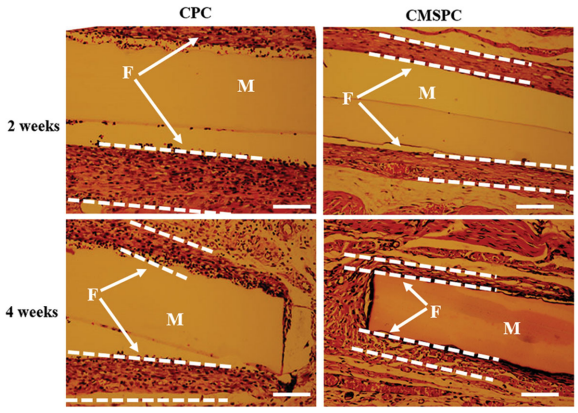

Figure 13. In vivo inflammatory response evaluation of CMSPC hybrid elastomers. Representative pictures indicating the H&E stained histological sections of the subcutaneous tissue surrounding CPC and CMSPC hybrid polymers after 2 and 4 weeks in vivo (M: materials; F: fibrous capsule, Scale bar: 100 μm). CPC elastomeric polymer was used as control. CMSPC hybrid elastomers demonstrated decreased fibrous capsule formation when compared to pure CPC control, indicating their low inflammation responses.

4. Experimental Section

Materials: All chemicals were purchased from Sigma-Aldrich unless otherwise noted and used without further purification.

Synthesis of Multifunctional Silica-Poly(citrates) (MSPC) Hybrid Prepolymers: The MSPC hybrid prepolymers were synthesized by polymerization reaction of 1,8-octanediol (OD), citric acid (CA), and (3-aminopropyl) triethoxysilane (AS) in 50 mL flask with mol rations of 1.0:1.0:0.2 and 1.0:1.0:0.4.[28] Briefly, the hybrid monomers were then melted at 160 °C under a constant flow of nitrogen gas while stirring, and reacted at 140 °C for further 60 min under stirring. After washing by deionized water and free drying, the MSPC hybrid prepolymers were stored for further use. The as-prepared MSPC prepolymers were denoted as MSPC0.2, MSPC0.3, and MSPC0.4 where 0.2 or 0.4 represents as the mole ratio of AS/citric acid. Pure PC prepolymer was also synthesized used as a control, according to the similar procedure.

Fabrication of Chemically Cross-Linked MSPC Hybrid Elastomers: The CMSPC hybrid elastomers were fabricated by conventional solvent casting and hexamethyl diisocyanate (HDI) cross-linking methods. Briefly, MSPC prepolymers (1.2 g) were dissolved in 12 mL of dimethylsulfoxide (DMSO) or dimethylformamide (DMF) and then reacted with different molar ratios of 1,6-hexamethyl diisocyanate to

residual hydroxyls of prepolymer (0.3, 0.5, and 0.6), using stannous octoate as a catalyst (0.1 wt%) at 55 °C for 2 h under constant stirring. The mixture was cast into a Teflon mold and allowed to dry until all the solvents evaporated at room temperature. To obtain the CMSPC hybrid elastomers, the resulting dried hybrids were put into an oven to postpolycondensation at 60,80,and 100 °C for 2 d. The pure cross-linked poly(citrates) (CPC) elastomers were used as a control and fabricated by a similar process. The final hybrid elastomers were denoted as CMSPC(X)-H(Y)-Z, where X, Y, and Z represent moral ratio of AS, HDI, and curing temperature, respectively.

Structural Characterizations of MSPC Hybrid Prepolymers and CMSPC Elastomers: The molecular structure of MSPC hybrid prepolymers was analyzed by nuclear magnetic resonance spectra (^{1}H NMR) (Ascend 400 MHz NMR, Bruker, Germany), using tetra-methyl-silane (0.00 ppm) as the internal reference. The characteristic peaks of different hybrid elastomers were assigned to be as follows. ^{1}H NMR (PC) (400 MHz, DMSO-d_6) δ/ppm: 1.27 (32H, s, —C$\underline{H_2}$C$\underline{H_2}$—), 1.36–1.62 (17H, m, —C$\underline{H_2}$CH$_2$O—), 2.62–2.89 (16H, m, —OCOC$\underline{H_2}$COH), 3.92–4.08 (14H, m, —CH$_2$C$\underline{H_2}$O—), 5.16–5.64 (4H, m, —OCOC$\underline{H_2}$CO—). ^{1}H NMR (MSPC) (400 MHz, DMSO-d_6) δ/ppm: 0.42–0.62 (2H, m, —NHCH$_2$C$\underline{H_2}$CH$_2$Si—), 1.16 (2H, t, —NHCH$_2$CH$_2$C$\underline{H_2}$Si—), 1.26 (40H, s, —C$\underline{H_2}$C$\underline{H_2}$—), 1.37–1.62 (22H, m, —C$\underline{H_2}$CH$_2$O—), 2.61–2.89 (16H, m, —OCOC$\underline{H_2}$COH), 3.92–4.07 (12H, m, —CH$_2$C$\underline{H_2}$O—), 4.35 (2H, s, —NHC$\underline{H_2}$CH$_2$CH$_2$Si—), 7.52 (1H, s, —N$\underline{H}$CH$_2$CH$_2$CH$_2$Si—). The average molecular weight of MSPC hybrids was analyzed by gel permeation chromatography (GPC) (E2695, Waters, USA). Fourier transform infrared (FTIR) spectra were obtained at room temperature using a (Nicolet 6700 FTS40, Thermo Scientific Instrument, USA). The spectra were recorded in the range of 4000–600 cm^{-1} at a resolution of 4 cm^{-1}. The surface microstructure and nanostructure of hybrid elastomers were evaluated by field emission scanning electron microscope (FE-SEM, SU8010, Hitachi, Japan) and transmitted electron microscope (TEM, H-8000, Hitachi, Japan). For TEM test, the samples were freezed and cut into a section with a thickness of 60–100 nm using a cryosection system (Leica EM FC7, Leica, Germany). The elemental composition of hybrids was measured through energy dispersive spectroscopy (EDS) analysis on the SEM.

Thermal Properties Evaluation of CMSPC Hybrid Elastomers: Differential scanning calorimetry (DSC) (DSC-60A, SHIMADZU, Japan) and thermogravimetric analysis (TGA) (Q500, TA, USA) were employed to investigate the thermal change and stability of hybrid elastomers. The glass transition temperature (T_g) was determined based on the DSC curves. The thermal decomposition process was monitored by TGA thermograms at a scanning speed of 10 °C min^{-1} in the range of 50 °C–700 °C. The temperature at which 10% mass loss happened was defined as the decomposition temperature (T_d).

Mechanical Properties Investigation of CMSPC Hybrid Elastomers: The stress–strain behavior, elongation at break and elastic modulus of elastomers were conducted by uniaxial tensile test on a mechanical testing machine and TestWorks4 software (Criterion Model 43, MTS, MN). Briefly, CMSPC elastomers films were cut to a size of 60 mm × 6 mm (length × width) and tested at a rate of 50 mm min^{-1}. The stress–strain curves and the tensile stress (MPa) were determined from applied force (N) and cross section area (mm^2). The elongation at break was obtained by calculating film length in tensile test. The slope of stress–strain curve at 5% of strain was defined as the Young's modulus of samples. At least four species per sample were tested to obtain the mean value and standard deviation. The antifatigue mechanical behavior was evaluated by tensile loading repeatedly for several times.

Hydrophilicity, pH Stability, and Degradation Analysis of CMSPC Hybrid Elastomers: The hydrophilicity of hybrid elastomers was determined by testing the water contact angles at room temperature using a goniometer and imaging system (SL200KB, Kino, USA). The water contact angles were obtained after water dropping for different period of times. At least four independent tests at different positions were carried out. The solution pH after samples soaking in phosphate buffer solution (PBS) was tested by a pH meter (5 mg mL^{-1}). The pH evaluation was done by a static (without PBS refreshing) and dynamic test (refreshing at time points). The in vitro degradation for a short time was carried out in 0.05 N NaOH solution at a sample concentration of 5 mg mL^{-1}. At least four species per sample were tested.

Photoluminescent Studies of MSPC and CMSPC Hybrids: The photoluminescent properties including excitation and emission spectra were carried out by a fluorescence spectrometer (F-4600, HITACHI, Japan) at room temperature. The excitation and emission slit widths for all samples were chose as 5 nm. The emission spectra of PC and MSPC were tested by dissolving them in DMSO (1 wt%). The highly tunable fluorescent properties were evaluated by determining the emission spectra with different excitation wavelengths. The fluorescent pictures of prepolymer solution and elastomeric films samples were obtained under excitation at 365 nm using ultraviolet lamp.

Antibacterial Studies of MSPC and CMSPC Hybrids: Staphylococcus aureus was provided kindly by department of microbiology, the first affiliated hospital, Xi'an Jiaotong University, P. R. China. The bacteria were cultured in tryptic soy broth. The antibacterial ability of hybrid elastomers was evaluated by soaking samples into solution containing *S. aureus* with a concentration of 1×10^5 for different times. At each time point, the optical density of microorganism solutions was determined by a microplate reader as a function of time (SpectraMax i3, Molecular Devices, USA). The broth containing bacterials was used as a control. The killing percent was defined as the relative intensity with control. At least four times per sample were repeated.

In Vitro Osteoblasts Attachment and Proliferation: The osteoblasts (MC3T3-E1) were used to determine the cellular biocompatibility of CMSPC hybrid elastomers. All cells were cultured in a Dulbecco's modified Eagle's medium (DMEM, Invitrogen) with 10% (v/v) fetal bovine serum at an atmosphere of 5% CO_2 at 37 °C. The medium was changed every the other day. The CPC and CMSPC elastomers (10 mm × 10 mm) after sterilization were put in a 24-well tissue culture plate (TCP). Cells were seeded on materials surface with a density of 4000 cells cm^{-2}, and cultured for 1, 3, and 5 d in growth medium. The cell attachment morphology was determined by fluorescent staining using calcein AM according to the instructions of product (Molecular Probes). The stained cells images were obtained from fluorescent microscope (BX51, Olympus, Japan). The cell viability and proliferation were determined by Alamar blue kit (Invitrogen). Briefly, at each culture time, the 10% v/v Alamar blue fluorescent dye was added into the growth media containing cells and incubated for 4 h. The cell viability was determined by testing the fluorescent intensity using a microreader (SpectraMax i3, Molecular Devices, USA). The medium containing 10% Alamar blue or materials was used as a control. At least four species for each sample were analyzed to obtain the mean value and standard deviation.

Alkaline Phosphatase Activity Evaluation: The osteogenic differentiation of cells was determined by ALP activity evaluation. The CPC and CMSPC hybrid elastomers films were placed in 12-well plates and seeded with osteoblasts (MC3T3-E1) at a density of 1.6×10^4 cells well^{-1}. The tissue culture plates without adding samples, CPC elastomers and commercial poly(lactic-*co*-glycolic acid) (PLGA, 50/50), were used as a control. The intracellular ALP activities of MC3T3 were evaluated by SensoLyte pNPP Alkaline Phosphatase Assay Kit (Ana Spec, USA) after culture on elastomers for 7 and 14 d. At least four species per sample were tested. The ALP activities were normalized to the total protein content tested by the Pierce bicinchoninic acid (BCA) Protein Assay Kit (Thermo, US) according to the manufacturer's instructions.

Extracellular Matrix Biomineralization Analysis: The extracellular matrix biomineralization was assayed by von Kossa staining kit (Genmed, China) according to the manufacturer instructions. Briefly, after culture for 14 d on elastomer surfaces, samples including cells were gently rinsed twice with Reagent A, fixed in Reagent B for 15–20 min, and washed with Reagent A twice again. Finally, they were stained with Reagent C for 30 min in the dark and exposed to an incandescent lamp (100 W) for 30 min. The calcium biomineralization pictures were obtained by a microscope (Olympus IX53).

Osteoblastic Genes Expression Investigations: Gene expression of ALP, OCN (osteocalcin), OPN (osteopotin), and RUNX-2 (runt-related transcription factor 2) from the cells after cultured for 1, 2,

Table 2. Primer pairs of real-time PCR used in present study.

Gene	Forward primer (F) and reverse primer (R) (5′-3′)	Size [bp]	Annealing temperature [°C]
ALP	F: CCAACTCTTTTGTGCCAGAGA	110	61
	R: GGCTACATTGGTGTTGAGCTTTT		
OCN	F: AACATAGTGTCGTCGTTTCTTTCTG	179	60
	R: GGCGTGGCATCTGTGAGGT		
OPN	F: TCTTCCCAAAGCCAGAGCG	107	65
	R: TGCCATTCGAGGTGGTCG		
RUNX-2	F: TAAGAAGAGCCAGGCAGGTG	111	58
	R: TAGTGCATTCGTGGGTTGG		
GAPDH	AGGTCGGTGTGAACGGATTTG	123	61
	R: TGTAGACCATGTAGTTGAGGTCA		

and 3 weeks was detected by quantitative real-time polymerase chain reaction (Q-RT-PCR). At determined culture period, the cultured cells with materials were rinsed for twice by PBS and total RNA was extracted using the TRIzol assay kit (Life technologies, USA). The RNA concentrations were quantified using the Nanodrop reader system (Thermal Sci, USA). The first strand was synthesized according to the manufacturer's instructions. The cycle parameters for the RT reaction were 43 °C for 1 h and 70 °C for 10 min. The Q-RT-PCR was set up in a 15 μL mixture containing 7.5 μL iTaq Universal SYBR Green Supermix (Bio-rad, USA), 6.4μL ddH_2O, 0.5 μL cDNA template, 0.3 μL forward primer, and 0.3 μL reverse primer. The amplification parameters were 94 °C for 5 min, followed by 30 cycles of 94 °C for 30 s, 57 °C for 30 s, and 72 °C for 30 s. All data were analyzed using 2-ΔΔ Ct method. Glyceraldehyde 3-phosphate dehydrogenase (GAPDH) was used as a housekeeping gene for PCR amplification. The primer pairs used in this study are shown in **Table 2**.

In Vivo Immunological Response after Implantation: All animals used in this study were obtained from Xi'an experimental animal company (6 weeks, male, 180–200 g) under guidelines of Animal Care and Use Committee, Xi'an Jiaotong University. After anesthesia with 10% chloral hydrate, a dorsal incision about 1 cm was carried out on rats to create a subcutaneous pocket for materials implantation. The CPC and CMSPC hybrid elastomers were cut into films with a size of 5 mm × 3 mm and sterilized by UV irradiation. After transplantation for 2 and 4 weeks, the elastomers were harvested for further histological analysis. No obvious immunological or infectious complications were observed throughout the experiments. The rats without any implants but undergoing the same surgical procedure were used as sham controls. At the predetermined time, the implants were retrieved and fixed in a formaldehyde fixative at room temperature for 3 d. For histological analysis, the fixed implants were embedded in paraffin and sectioned. The paraffin sections of subcutaneous explants were stained with hematoxylin-eosin (H&E). The stained sections were examined by a microscope (Olympus, Japan).

Statistical Methods: Data are expressed as mean ± SD. Analysis was performed using the Statistical Program for Social Science for Windows. Results were made using student's *T*-test (two tail, unequal variance) and analysis of variance. A *p*-value of <0.05 was considered to be statistically significant.

Supporting Information

Supporting Information is available from the Wiley Online Library or from the author.

Acknowledgements

Y.D. and M.Y. contributed equally to this work. The valuable comments of potential reviewers are acknowledged. This work was supported by the scientific research starting foundation from Xi'an Jiaotong University, the Natural Science Basic Research Plan in Shaanxi Province of China (Program No. 2015JQ5165), the Fundamental Research Funds for the Central Universities (XJJ2014090), National 973 Project of China (2012CB619100), and National Natural Science Foundation of China (51372005).

Received: April 28, 2015
Revised: June 15, 2015
Published online: July 14, 2015

[1] D. Bliuc, N. Nguyen, D. Alarkawi, T. Nguyen, J. Eisman, J. Center, *Osteoporosis Int.* **2015**, *26*, 1331.
[2] S. Dimmeler, S. Ding, T. A. Rando, A. Trounson, *Nat. Med.* **2014**, *20*, 814.
[3] Q. Zhang, V. N. Mochalin, I. Neitzel, K. Hazeli, J. Niu, A. Kontsos, J. G. Zhou, P. I. Lelkes, Y. Gogotsi, *Biomaterials* **2012**, *33*, 5067.
[4] Q. Zhang, V. N. Mochalin, I. Neitzel, I. Y. Knoke, J. Han, C. A. Klug, J. G. Zhou, P. I. Lelkes, Y. Gogotsi, *Biomaterials* **2011**, *32*, 87.
[5] J. I. Dawson, J. Kanczler, R. Tare, M. Kassem, R. O. Oreffo, *Stem Cells* **2014**, *32*, 35.
[6] P. Zhou, Y. Xia, X. Cheng, P. Wang, Y. Xie, S. Xu, *Biomaterials* **2014**, *35*, 10033.
[7] A. C. Akyildiz, L. Speelman, F. J. Gijsen, *J. Biomech.* **2014**, *47*, 773.
[8] X. Ojanen, H. Isaksson, J. Töyräs, M. Turunen, M. Malo, A. Halvari, J. S. Jurvelina, *J. Biomech.* **2015**, *48*, 269.
[9] L. M. Mathieu, T. L. Mueller, P.-E. Bourban, D. P. Pioletti, R. Müller, J.-A. E. Månson, *Biomaterials* **2006**, *27*, 905.
[10] E. Giesen, M. Ding, M. Dalstra, T. Van Eijden, *J. Biomech.* **2001**, *34*, 799.
[11] T. R. Nayak, H. Andersen, V. S. Makam, C. Khaw, S. Bae, X. Xu, P.-L. R. Ee, J.-H. Ahn, B. H. Hong, G. Pastorin, B. Özyilmaz, *ACS Nano* **2011**, *5*, 4670.
[12] J. R. Jones, *Acta Biomater.* **2013**, *9*, 4457.
[13] B. Lei, K. H. Shin, Y. W. Moon, D. Y. Noh, Y. H. Koh, Y. Jin, H. Y. Kim, *J. Am. Ceram. Soc.* **2012**, *95*, 30.
[14] U. Ripamonti, L. C. Roden, L. F. Renton, *Biomaterials* **2012**, *33*, 3813.
[15] H. Liu, G. W. Xu, Y. F. Wang, H. S. Zhao, S. Xiong, Y. Wu, B. C. Heng, C. R. An, G. H. Zhu, D. H. Xie, *Biomaterials* **2015**, *49*, 103.
[16] B. Lei, L. Wang, X. Chen, S.-K. Chae, *J. Mater. Chem. B* **2013**, *1*, 5153.
[17] Y. Zhang, R. T. Tran, I. S. Qattan, Y.-T. Tsai, L. Tang, C. Liu, J. Yang, *Biomaterials* **2013**, *34*, 4048.
[18] Z. W. Xie, Y. Zhang, L. Liu, H. Weng, R. P. Mason, L. P. Tang, K. T. Nguyen, J.-T. Hsieh, J. Yang, *Adv. Mater.* **2014**, *26*, 4491.
[19] Y. Zhang, J. Yang, *J. Mater. Chem. B* **2013**, *1*, 132.
[20] A. Jacombs, S. Tahir, H. Hu, A. K. Deva, A. Almatroudi, W. L. Wessels, D. A. Bradshaw, K. Vickery, *Plast. Reconstr. Surg.* **2014**, *133*, 471.
[21] B. A. Lipsky, G. J. Moran, L. M. Napolitano, L. Vo, S. Nicholson, M. Kim, *BMC Infect. Dis.* **2012**, *12*, 227.
[22] F. Andrade, D. Rafael, M. Videira, D. Ferreira, A. Sosnik, B. Sarmento, *Adv. Drug Delivery Rev.* **2013**, *65*, 1816.
[23] Q. Yu, Z. Wu, H. Chen, *Acta Biomater.* **2015**, *16*, 1.
[24] J. Yang, A. R. Webb, G. A. Ameer, *Adv. Mater.* **2004**, *16*, 511.

[25] R. A. Hoshi, R. Van Lith, M. C. Jen, J. B. Allen, K. A. Lapidos, G. Ameer, *Biomaterials* **2013**, *34*, 30.
[26] A. Silvestri, M. Boffito, S. Sartori, G. Ciardelli, *Macromol. Biosci.* **2013**, *13*, 984.
[27] J. Yang, Y. Zhang, S. Gautam, L. Liu, J. Dey, W. Chen, R. P. Mason, C. A. Serrano, K. A. Schug, L. Tang, *Proc. Natl. Acad. Sci. U.S.A.* **2009**, *106*, 10086.
[28] Y. Du, J. Ge, Y. Shao, P. X. Ma, X. Chen, B. Lei, *J. Mater. Chem. B* **2015**, *3*, 2986.
[29] B. Lei, X. Chen, X. Han, J. Zhou, *J. Mater. Chem.* **2012**, *22*, 16906.
[30] Q. Chen, S. Liang, G. A. Thouas, *Prog. Polym. Sci.* **2013**, *38*, 584.
[31] Y. Xue, L. Wang, Y. Shao, J. Yan, X. Chen, B. Lei, *Chem. Eng. J.* **2014**, *251*, 158.
[32] B. Lei, K.-H. Shin, I.-H. Jo, Y.-H. Koh, H.-E. Kim, *Mater. Chem. Phys.* **2014**, *145*, 397.
[33] X. Zhao, Y. Wu, Y. Du, X. Chen, B. Lei, Y. Xue, P. X. Ma, *J. Mater. Chem. B* **2015**, *3*, 3222.
[34] L. M. Mathieu, T. L. Mueller, P.-E. Bourban, D. P. Pioletti, R. Müller, J.-A. E. Månson, *Biomaterials* **2006**, *27*, 905.
[35] E. Giesen, M. Ding, M. Dalstra, T. Van Eijden, *J. Biomech.* **2001**, *34*, 799.
[36] J. Dey, H. Xu, J. Shen, P. Thevenot, S. R. Gondi, K. T. Nguyen, B. S. Sumerlin, L. Tang, J. Yang, *Biomaterials* **2008**, *29*, 4637.
[37] M. Chen, M. Yin, *Prog. Polym. Sci.* **2014**, *39*, 365.
[38] E. Carlisle, in *Silicon and Siliceous Structures in Biological Systems* (Eds: T. L. Simpson, B. E. Volcani), Springer, New York, USA **1981**, pp 69–94.
[39] D. Arcos, M. Vallet-Regí, *Acta Biomater.* **2010**, *6*, 2874.
[40] L. L. Hench, in *Advances in Calcium Phosphate Biomaterials* (Ed: B. Ben-Nissan), Springer, Berlin, Germany **2014**, pp 51–70.
[41] M. Y. Shie, S. J. Ding, *Biomaterials* **2013**, *34*, 6589.
[42] H. Gu, F. Guo, X. Zhou, L. Gong, Y. Zhang, W. Zhai, L. Chen, L. Cen, S. J. L. Cui, *Biomaterials* **2011**, *32*, 7023.
[43] M. J. N. Pereira, B. Ouyang, C. A. Sundback, N. Lang, I. Friehs, S. Mureli, I. Pomerantseva, J. McFadden, M. C. Mochel, O. Mwizerwa, P. D. Nido, D. Sarkar, P. T. Masiakos, R. Langer, L. Ferreira, J. M. Karp, *Adv. Mater.* **2013**, *25*, 1209.